

Scaling Effect in DEM Simulations of Direct Shear Test

S. Ji, H H Shen, and A. Orlando

Civil & Environmental Eng., Clarkson University, 132 Rowley, Civil and Environmental Eng. Dept.,
Clarkson University, Potsdam, NY 13699-5710

ABSTRACT

For quasi-static applications such as land subsidence or the initial stage of embankment failure, the rate effect is small. In these cases the bulk friction of the granular material is most conveniently obtained by a direct shear test. However, commercially available direct shear apparatus are small in relation to particle size for a wide range of applications. In parallel with this situation, granular materials handling systems face more troubles than their fluid counterparts. Numerical simulations of granular systems offer a way to make improvements. Constrained by the simulation time requirement, much smaller number of particles than reality can be incorporated in these simulations. As a result, either the size of the equipment has to be reduced, or the size of the particles has to be enlarged in these simulations. To investigate the possibility of using direct shear apparatus for a wider range of particles, and to shed some light on scaling laws for such an apparatus, a direct shear test is performed in this study using Discrete Element Models to study the scaling effect. It is found that by scaling properly, it is possible to use direct shear box for bulk friction measurement when the size of the box is roughly 10 times the particles size. It is also shown that overburden plays an important role in the bulk friction. Lastly, it is surprising to observe that contact friction affects the scaling law in such a way that the lower the contact friction, the more dependent the bulk friction is to the shear box size.

KEYWORDS: Granular Materials, Scaling, DEM Simulation, Shear Box.

I. Introduction

Computational tools for engineering design involving liquid and gases are mature enough to replace traditional physical tests in many cases. For solid handling there is still a long way to go to achieve this goal. The lack of constitutive law forces a direct simulation of each individual particle in a large system. Limited by computing power the number of particles that can be handled in realistic time is much lower than in physical tests. Therefore a scaling law is needed to bridge the results from a small number of particles to reality. One of the most important parameters in granular mechanics is the bulk friction coefficient.

A direct shear box is a standard apparatus used to measure shear strength parameters and expansion properties of soil, rock, sand, and other granular materials (some recent works include: Abou-Chakra and Tuzun, 1999; Dittes and Labuz, 2002; Ling and Dietz, 2004). The most significant advantages of the direct shear box are that it is simple to build and operate, and tests can be performed in a short time. However shortcomings are that the deformation and stress fields are strongly non-uniform in the material, contact area diminishes during shearing, stress concentrations occur at ends, principle stresses are not known, and rotation of the top loading plate takes place (Tejchman, 2005). Some continuum numerical simulations of direct shear tests were carried out in the past decade (Cividini and Gioda, 1992; Tejchman, 2005). Recently, the 2D Discrete Element Model (DEM) was adopted in the direct shear tests (Thornton and Zhang, 2003).

Disks, spheres, or ellipses, are commonly used in the (DEM) to simulate granular materials. However these ideal shapes do not describe the real granular materials well. By bonding or clumping disks or spheres together, different particle shapes were generated to create realistic shapes (e.g. Peters and Dziugys, 2002; Cheng et al., 2003). In this study, a paired particle with 25% or 50% overlap is constructed to model the irregularity of real granular materials. We will study the scaling effect in direct shear tests of these clumped particles. The quaternion method will be adopted to simulate the rotation of the clumps between local and global coordinates.

II. Discrete Element Model with Clumped particles

In the DEM simulation of clumped particles, the local coordinate system is more convenient to model particle rotation, and the global coordinate system is used to define the particle location, and the particle interaction. The notations and relations between the local and global coordinates of one clumped particle are shown in Fig. 1. The global and local coordinates have also been called as space and body frames.

If a clumped-particle is formed with overlapping spheres, its total mass, center of mass, and moment of inertia are difficult to calculate analytically. Here, a numerical method is adopted. The strategy is to first define a domain large enough to contain the clump, and numerically the clump is discretized into small cubes of volume $\Delta x \times \Delta y \times \Delta z$. For each cube we detect if it is inside the clump by measuring the distance between the cube and the centers of the spheres. The contribution of the mass and moment of inertia is accumulated from each of the small cubes that are inside the clump. With this method, the total mass,

mass center and moment of inertia can be determined with

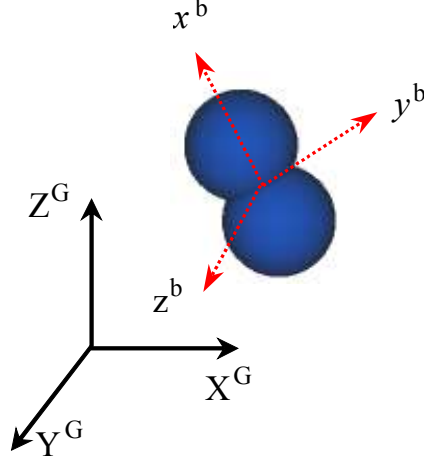


Fig. 1 Local and global coordinates in the DEM simulation of clumped particles.

$$\tilde{M} = \rho \sum_{k=1}^K \Delta V_k \quad (1)$$

$$\tilde{X}_i = \frac{\rho \sum_{k=1}^K x_{ki} \Delta V_k}{M} \quad (2)$$

$$\tilde{I}_{ii} = \rho \sum_{k=1}^K (\tilde{X}_j - x_j^k)^2 \quad (3)$$

The accuracy of the numerical results increases with decreasing cube size. When we set $\Delta x = \Delta y = \Delta z = D_{\min}/20$, the calculated clump mass, mass center and moment of inertia are compared with the analytical solution for simple cases of none overlapping spheres. The precision was found to be higher than 99%.

With the quaternion method, the torque, rotational velocity and other vectors can be transformed from the rotating local frame to a global frame. If the orientation of a clump is specified, the relation between the fixed space system \mathbf{e}^s and the moving body system \mathbf{e}^b is linked by the rotation matrix \mathbf{A} (Allen and Tildesley, 1987)

$$\mathbf{e}^b = \mathbf{A} \cdot \mathbf{e}^s \quad (4)$$

$$\mathbf{e}^b = \mathbf{A}^T \cdot \mathbf{e}^s \quad (5)$$

The rotation matrix satisfies $\mathbf{A}^{-1} = \mathbf{A}^T$. The matrix \mathbf{A} can be determined with Euler angles or quaternions. A quaternion \mathbf{Q} is a set of four scalar quantities

$$\mathbf{Q} = (q_0, q_1, q_2, q_3) \quad (5)$$

which satisfy the constraint

$$q_0^2 + q_1^2 + q_2^2 + q_3^2 = 1 \quad (6)$$

In terms of the quaternions, the rotation matrix can be written as

$$\mathbf{A} = \begin{pmatrix} q_0^2 + q_1^2 - q_2^2 - q_3^2 & 2(q_1q_2 + q_0q_3) & 2(q_1q_3 - q_0q_2) \\ 2(q_1q_2 - q_0q_3) & q_0^2 - q_1^2 + q_2^2 - q_3^2 & 2(q_2q_3 + q_0q_1) \\ 2(q_1q_3 + q_0q_2) & 2(q_2q_3 - q_0q_1) & q_0^2 - q_1^2 - q_2^2 + q_3^2 \end{pmatrix} \quad (7)$$

In the body frame, the rotational acceleration becomes

$$\dot{\omega}_x^b = \frac{M_x^b}{I_{xx}} + \left(\frac{I_{yy} - I_{zz}}{I_{zz}} \right) \omega_y^b \omega_z^b \quad (8)$$

$$\dot{\omega}_y^b = \frac{M_y^b}{I_{yy}} + \left(\frac{I_{zz} - I_{xx}}{I_{yy}} \right) \omega_z^b \omega_x^b \quad (9)$$

$$\dot{\omega}_z^b = \frac{M_z^b}{I_{zz}} + \left(\frac{I_{xx} - I_{yy}}{I_{zz}} \right) \omega_x^b \omega_y^b \quad (10)$$

where I_{xx} , I_{yy} , and I_{zz} are the three principal moments of inertia in the body frame. The moment in the body frame is related to that in the space frame by

$$\begin{pmatrix} M_x^b \\ M_y^b \\ M_z^b \end{pmatrix} = \mathbf{A} \begin{pmatrix} M_x^s \\ M_y^s \\ M_z^s \end{pmatrix} \quad (11)$$

here M_x^b , M_y^b and M_z^b are the moments in the body frame, and M_x^s , M_y^s and M_z^s are the moments in the space frame. The moments in the space frame can be determined from collisions with other clumps.

When the rotational velocity in a body frame is calculated, the rotational velocity in a space frame can be transformed as

$$\begin{pmatrix} \omega_x^s \\ \omega_y^s \\ \omega_z^s \end{pmatrix} = \mathbf{A}^T \begin{pmatrix} \omega_x^b \\ \omega_y^b \\ \omega_z^b \end{pmatrix} \quad (12)$$

The quaternions for each clump satisfy the equation of motion (Allen and Tildesley, 1987; Kosenko, 1998)

$$\begin{pmatrix} \dot{q}_0 \\ \dot{q}_1 \\ \dot{q}_2 \\ \dot{q}_3 \end{pmatrix} = \frac{1}{2} \mathbf{W} \begin{pmatrix} 0 \\ \omega_x^b \\ \omega_y^b \\ \omega_z^b \end{pmatrix} \quad \text{where } \mathbf{W} = \begin{pmatrix} q_0 & -q_1 & -q_2 & -q_3 \\ q_1 & q_0 & -q_3 & q_2 \\ q_2 & q_3 & q_0 & -q_1 \\ q_3 & -q_2 & q_1 & q_0 \end{pmatrix} \quad (13)$$

With the conversion between the global and local coordinates described above, the motion, especially the rotation of clumped particles, can be simulated using an explicit finite difference scheme.

III. DEM Simulation of Direct Shear Tests of Clumped Particles

The direct shear apparatus includes an upper box and a lower box, separated by a small gap. At the top of the upper box a floating plate is applied which is free to move vertically. A normal load may be applied to the floating plate to simulate different overburden conditions. The lower box is subject to a prescribed constant velocity in the horizontal direction. Fig. 2 shows the schematics of this apparatus.

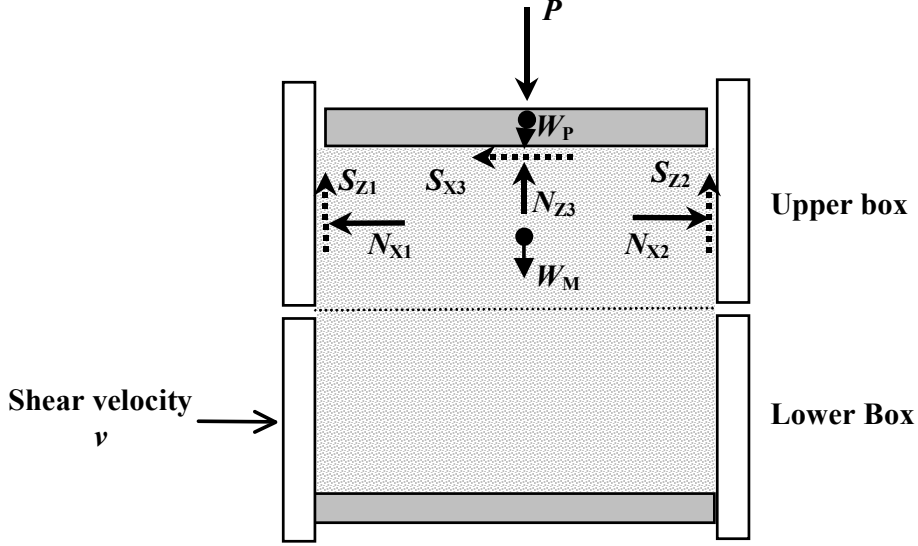


Fig. 2 Sketch of Forces applied on the upper shear box.

Because of the geometry, the shear plane of the granular material resides in the gap between the top and bottom half of the apparatus. On this plane, the normal force is the sum of the normal load P , the weight of the floating plate, and the weight of the granular materials in the upper box. The shear force can be found from the force balance between the sum of normal forces on the left and right walls and the shear forces on the floating top plate and the front and back side walls, as shown in Fig. 2. Therefore, on the shear plane, we have

$$F_N = P + W_P + W_M \quad F_S = \sum_{iw=1}^{N_{\text{wall}}} (N_{x_i} + S_{x_i}) \quad (14)$$

where F_N and F_S are the normal and shear force acting on the shear plane, respectively. P is the external normal load, W_P and W_M are the weight of the floating plate and the weight of the interior particles in the upper box. $N_{x_{iw}}$ and $S_{x_{iw}}$ are the normal and shear force in x direction between the particles and inside wall i of upper box. There are four side walls and one top wall in the upper box, and the total wall number $N_{\text{wall}} = 5$. The normal and shear stresses are

$$\sigma_{zz} = \frac{F_N}{LB} \quad \sigma_{xz} = \frac{F_S}{LB} \quad (15)$$

where L and B are the length and width of the box cross-section respectively. The bulk friction coefficient on the shearing plane is

$$\mu_b = \frac{\sigma_{zz}}{\sigma_{zz}} = \frac{F_N}{F_S} \quad (16)$$

To initiate the simulation of a packed granular material, the particles are set to half of their real size initially, so that a random distribution with desired number of particles is possible. After the packing, the particles grow to the final size slowly. In the growth process, the particles contact each other to re-organize their location and orientation automatically. After the growth phase, the external normal load is applied on the top plate to further pack the particles. The shear process starts when the particles come to a steady state under this normal load. Therefore, we have mainly three stages in the shear test simulation - growth, loading and shear.

To study the scaling effect, dimensionless parameters are defined as $L^* = \frac{L}{D}$,

$$x^* = \frac{x}{D}, z^* = \frac{z}{D}, v^* = \frac{v}{\sqrt{Dg}}, E^* = \frac{E}{Dg\rho}, \sigma^* = \frac{\sigma}{Dg\rho}, \tau^* = \frac{\tau}{Dg\rho}. \text{ Here } L \text{ is the box size, } D$$

is the mean particle diameter, x is the horizontal shear displacement, z is the vertical displacement, v is the shear rate, E is the Young's modulus, g is gravity, ρ is the particle density, σ is the applied normal stress, and τ is the simulated shear stress. In the above, x, v, E, g, ρ, σ are input variables that can be assigned, and z and τ are dependent variables that result from the input. We first test the scaling effect by keeping the dimensionless parameters $L^*, x^*, v^*, E^*, \sigma^*$ constant, and using various particle diameters $D = \alpha D_0$ (here $\alpha = 0.1, 1, 10, 100$ and $D_0 = 7.31\text{mm}$) to simulate the shear stress and thus the bulk friction. The parameters used for scaling index $\alpha = 1.0$ are listed in Table 1. In the simulation, a uniformly distributed size from a minimum of $0.8D$ to a maximum of $1.2D$ is used to generate the clumping particles. Each clump consists of equal size pairs with a 25% overlap.

A snapshot of the simulation is given in Fig. 3. The simulated bulk friction and dimensionless vertical displacement versus shear distance are plotted in Fig. 3. When conducting the scaling tests, we used the following rules for keeping the dimensionless parameters constant in all tests: length factor $\sim \alpha$, area factor $\sim \alpha^2$, mass factor $\sim \alpha^3$, force factor $\sim \alpha^3$, stress factor $\sim \alpha$.

Table 1. Parameters used in the DEM simulation

Variables	Definition	Values
L, B	Upper and lower box Length, and width	10 cm
H_1, H_2	Upper and lower box height	3.71 cm
μ_p	Contact friction of particles	0.8
e_p	Restitution among particles	0.7
μ_{p-w}	Friction between particle and side wall	0.2
e_{p-w}	Restitution between particle and side wall	0.9
μ_{p-w}	Friction between particle and top/bottom porous cover	1.0
U	Shear velocity in experiment	10.0 mm/s

S	Shear deformation	10 mm
P	Normal load	500 N
M	Total Mass of shear materials	1.0 kg
m	Single Particle Mass	0.8 ~ 1.2 g
ρ	Density	$2.545 \times 10^3 \text{ kg/m}^3$
E	Young's modulus	58.0 MPa
N_c	Clump number	993

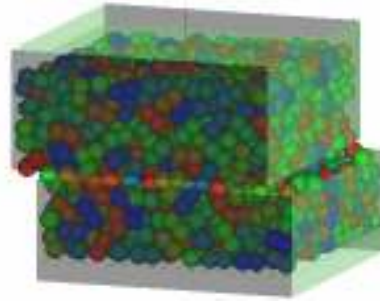


Fig. 3 A snapshot of the direct shear box filled with clumped-particles in the DEM simulation.

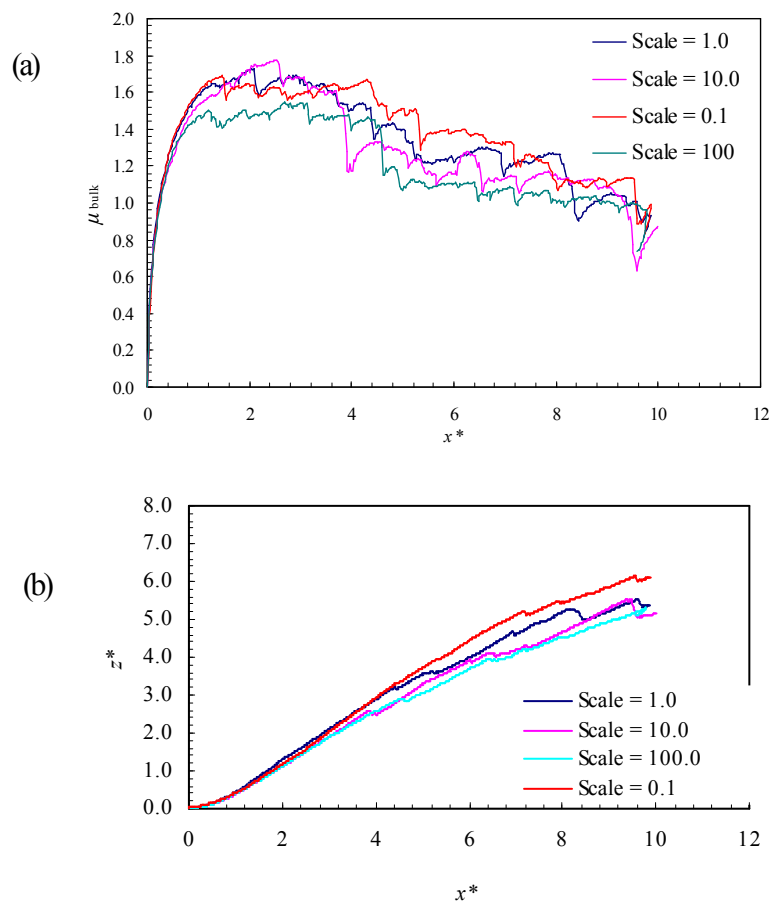


Fig. 4 (a) Bulk friction and (b) dimensionless vertical displacement results under various scales.

The shear induced expansion is obvious from Fig. 4(b). The dimensionless vertical displacements are very close under different scales. The bulk friction coefficients shown in Fig. 4(a) increase with the shear displacement, then approach their peaks at about 2. The

averaged bulk friction coefficients in the range from 2 ~ 3 are 1.60, 1.66, 1.72 and 1.50 when the scaling factor $\alpha = 0.1, 1, 10$ and 100, respectively. More tests were carried out with different initial packings. It was found that the simulated bulk friction had a variation around 10% of the mean, regardless of the scaling factor. Therefore, it can be concluded that the bulk friction coefficients are similar under various scales, provided that all dimensionless parameters are kept constant in different scales.

It is interesting to note that the bulk friction coefficient is about twice the contact friction between particles. Using single disk shaped particles, direct shear tests were performed to simulate sand (Thornton and Zhang, 2001). They found that by using a contact friction coefficient $\mu_p = 0.7$, the simulated bulk friction was around 0.46, less than the contact friction coefficient. Therefore, the added friction due to interlocking between these clumped particles is very significant. This additional friction cannot be modeled with spheres or disks.

Many granular material handling systems are built using smaller scale prototypes, where the normal load is drastically lower than the scaled-up facility. Therefore a natural question to ask is how the bulk friction depends on the overburden. In order to study the effect of overburden, we change the applied normal load but keep all other parameters constant. The scaling factor is fixed at $\alpha = 1.0$. The direct shear tests are simulated with σ equals to 5.0, 50, 500 and 5000 kPa under the action of normal loads of 50, 500, 5000 and 50000N, respectively. The other parameters are all keep constant except the external normal load. The simulated vertical displaces and bulk friction coefficients are plotted in Fig. 5. From the vertical displacements, the shear expansion is strongly dependent on the normal load. Not surprisingly the higher the normal load the smaller the expansion. Moreover, the bulk friction coefficient decreases with increasing normal stress. The phenomena have been observed in the lab tests of direct shear tests (Cividini and Gioda, 1992; Ling and Dietz, 2004).

The reason for scale dependence or the lack of such dependence is an interesting research topic. It is conceivable that granular materials possess other internal length scales than the most obvious one: the particle size. Therefore, there are other important length scales for granular material handling systems than L and D as listed in the beginning of this study. For a packed system, the most obvious candidate for this additional length scale is the force-chain (Peters et al., 2005) structure. In spite of lacking a quantitative description of a force chain, it is easy to imagine that as the scale of the box becomes small relative to the particles size, force chains may span the whole apparatus. When this happens the size of the apparatus will affect the result of the measurement. It is also easy to imagine that contact friction plays an important role in building the force chains in a granular material. Therefore we suspect that the scaling effect may be influenced by the contact friction. To study this, we investigate the direct shear results using different contact friction and different box size, while keeping the particle size constant. Namely, we change only L^* and μ_p , but keep ν^* , E^* , σ^* constant. In these simulations, the clumped particle is constructed with 50% overlap, the shear rate is 30 mm/s, and the Young's Modulus is 20 MPa. The other parameters are used as listed in Table 1. The results are shown in Fig. 6.

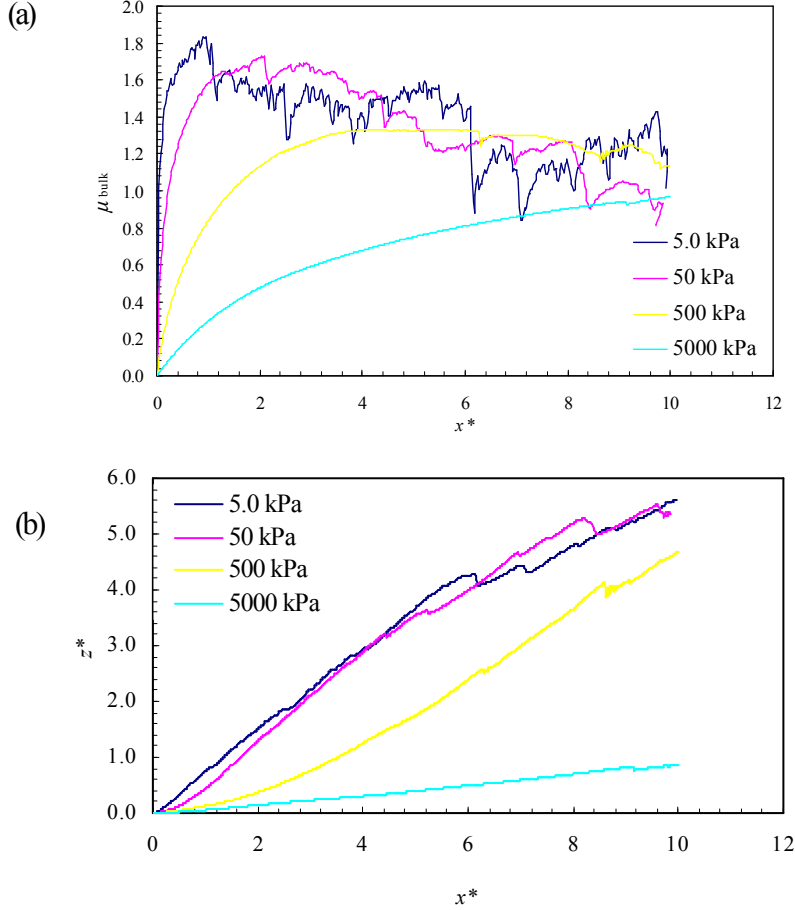


Fig. 5 (a) Bulk friction and (b) dimensionless vertical displacement results under different normal stresses.

From the results of Fig. 6, it is seen that as the box size increases, the bulk friction does approach a constant independent of the box size. Therefore, it is hopeful that direct shear test using small shear boxes may produce useful results for larger particles. It is also encouraging that DEM simulations that use large particles to simulate numerous small particles in a real system may also produce useful results, when proper scaling is used, such that scale dependence no longer play a role. However, it is surprising to see that no low contact friction, the scale dependence lasts longer than the higher friction cases. Our conjecture on the force chain apparently does not capture the complete picture of the internal length scale.

IV. Conclusions

The direct shear tests filled with clumped-particles were simulated under constant shear velocity and normal load with 3D DEM. It was found that under proper scaling, the bulk friction is independent of the scale of the apparatus. The normal load plays a significant role in the bulk friction, the higher the load the lower the bulk friction. Additional length scale was investigated by studying the bulk friction reaction to contact friction and shear box size. It was found that for each contact friction, there is a limiting size of the box, beyond which the box size no longer affect the bulk friction.

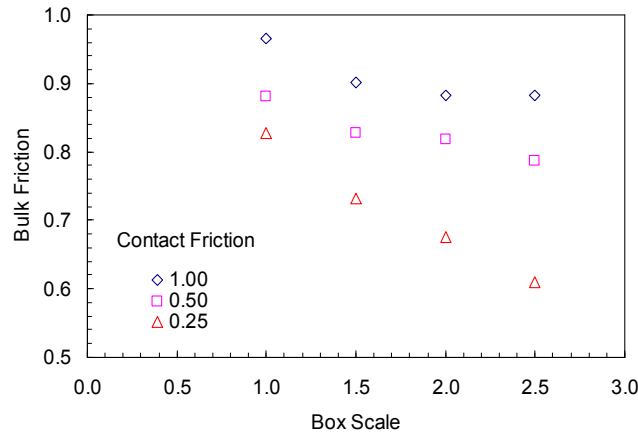


Fig. 6 Simulated bulk friction under different contact friction and box size.

V. Acknowledgements

This study is supported in part by NASA microgravity fluids program, Grant #NAG3-2717.

VI. References

1. Abou-Chakra H, Tuzun U. Coefficient of friction of binary granular mixtures in contact with a smooth wall Part I: direct shear box measurements of the effects of particle size ratio and particle surface roughness. *Chemical Engineering Science*, 1999, 54: 5901-5912.
2. Allen M P, Tildesley D J. *Computer simulation of liquids*. Oxford University Press (1987).
3. Cheng Y P, Nakata Y, Botton M D. Discrete element simulation of crushable soil. *Geotechnique*, 2003, 53(7): 633-641.
4. Cividini A, Gioda G. A finite element analysis of direct shear tests on stiff clays. *International Journal for Numerical and Analytical Methods in Geomechanics*, 1992, 16:869-886.
5. Dittes M, Labuz J F. Field and laboratory testing of St. Peter Sandstone. *Journal of Geotechnical and Geoenvironmental Engineering*, 2002, 128(5): 372-380.
6. Ling M L, Dietz M S. An improved direct shear apparatus for sand. *Geotechnique*, 2004, 54(4): 245-256.
7. Peters B, Dziugys A. Numerical simulation of the motion of granular material using object-oriented techniques. *Computer Methods in Applied Mechanics and Engineering*, 2002, 191: 1983-2007.
8. Peters J F, Muthuswamy M, Wibowo J, Tordesillas A. Characterization of force chains in granular material. *Physical Review E*, 2005, 72: 041307.
9. Tejchman J. FE analysis of shearing of granular bodies in a direct shear box. *Particulate science and Technology*, 2005, 23:229-248.
10. Thornton C, Zhang L. Numerical simulation of the direct shear test. *Chemical Engineering & Technology*, 2003, 26(2): 153-156.